Supplement of Atmos. Chem. Phys., 20, 6081–6094, 2020
https://doi.org/10.5194/acp-20-6081-2020-supplement

Atmospheric Chemistry and Physics
Open Access
EGU

Supplement of

A new marine biogenic emission: methane sulfonamide (MSAM), dimethyl sulfide (DMS), and dimethyl sulfone ($DMSO_2$) measured in air over the Arabian Sea

Achim Edtbauer et al.

Correspondence to: Achim Edtbauer (a.edtbauer@mpic.de)

Supplement

1 Deposition lifetime

The exchange flux F of various gases between an air and water interface can be predicted with the help of a two-layer model [5, 9, 10]:

$$F = K_G(G - \frac{A}{H}). \tag{1}$$

Where K_G is the overall mass-transfer coefficient (has dimensions of velocity), G is the gas phase concentration, A the aqueous phase concentration and H the Henry's law constant in the dimensionless form. If we assume that the aqueous phase concentration is zero (e.g. outside of the Somalia upwelling when traveling towards the ship) then equation 1 simplifies to:

$$F = K_G G. \tag{2}$$

The mass-transfer coefficient K_G can be expressed as:

$$\frac{1}{K_G} = \frac{1}{k_G} + \frac{1}{\frac{1}{4}\nu\alpha} + \frac{1}{Hk_L\beta}. \tag{3}$$

In this equation k_G is the gas phase and k_L the liquid phase mass-transfer coefficient, ν the mean molecular speed of the molecule, α the mass-accommodation coefficient and β an enhancement coefficient of the aqueous phase mass transfer flux due to removal of the molecule by chemical reactions. No enhancement means $\beta = 1$. The middle term which describes the interfacial resistance can be generally neglected in the natural environment because α is always sufficiently large [9]. If the molecule under investigation has a solubility of $H \gg H_{crit} = \frac{k_G}{k_L}$ then gas phase mass transport is dominant and the flux is independent of H. We determined a Henry's law constant in the range of $3.3 \times 10^4\,\mathrm{M\ atm^{-1}}$ - $6.5 \times 10^5\,\mathrm{M\ atm^{-1}}$ for methane sulfonamide (MSAM) (see Sect. S2) and for $DMSO_2$ literature indicates a value greater than $5 \times 10^4\,\mathrm{M\,atm^{-1}}$ [1]. This means that both are sufficiently soluble substances for which the assumption holds true that gas phase mass transport is controlling and the overall mass-transfer coefficient is given in the form:

$$\frac{1}{K_G} = \frac{1}{k_G}. \tag{4}$$

The gas phase mass-transfer coefficient for oceanic applications can be estimated with the help of the wind speed v [3]:

$$k_G = 0.0013v \tag{5}$$

for an observation height of 10 m which is the approximate height of observation during the AQABA campaign. The wind speed during the Arabian sea part in the second leg varied around $4\,\mathrm{m\ s^{-1}}$ and $14\,\mathrm{m\ s^{-1}}$ which yields: $K_G = 0.52\,\mathrm{cm\ s^{-1}}$ (v=$4\,\mathrm{m\ s^{-1}}$) and $K_G = 1.82\,\mathrm{cm\ s^{-1}}$ (v=$14\,\mathrm{m\ s^{-1}}$).
This in turn gives a lifetime (1/e) of 40 ± 14 hours for a wind speed of v=$4\,\mathrm{m\ s^{-1}}$ and about 11 ± 4 hours for v=$14\,\mathrm{m\ s^{-1}}$. The average marine boundary layer height used for the lifetime calculation was 750 ± 250 m.

2 Henry's law constant measurement

In order to resemble sea water more closely we added 35 g NaCl and 0.5 g $NaHCO_3$ to a combined volume of 1 L in MilliQ water. The obtained water is in the following referred to as sea water. Strictly speaking it does

not classify as artificial sea water because some ingredients like magnesium and calcium salts are missing. The MSAM mixing ratio of the headspace of 0.05 mol L^{-1} and 0.0005 mol L^{-1} MSAM in sea water, flushed with 100 ml min^{-1} of synthetic air (Air Liquide, Krefeld, Germany) each, was measured with a PTR-MS instrument. A range for the Henry's law constant was derived from these measurements as the ratio of the concentration of MSAM in solution (in M) vs. the measured partial pressure in the gas phase (in atm): 3.3×10^4 M atm^{-1} – 6.5×10^5 M atm^{-1}. Measurements were performed at 25° C and 995 mbar.

3 Weighting factors

Chlorophyll a water content encountered during transport of the airmasses towards the ship was weighted according to time before arrival at the ship. We employed a linear and an exponential weighting factor.

3.1 Linear weighting factors

The linear weighting factor is in the form $w = \frac{1}{1+p*t}$, where p is the weighting parameter and t is the number of hours before arrival at the ship's location. The *chlorophyll a* water content is multiplied by the weighting factor w to get the weighted *chlorophyll a* water content. We varied the p in the range from $p = 0.02$ to $p = 1$. The resulting plots are displayed in Fig. S1 till Fig. S4. A weighting parameter of $p = 0.02$ results in a high contribution and a $p = 1$ in a low contribution of *chlorophyll a* water content further away of the ship. Calculations of leg 1 with low weighting parameters $p = 0.02 - 0.1$ lead to a small increase in total *chlorophyll a* exposure of the trajectories (yellow lines in graphs) but no increase is seen when only the Somalia upwelling region is considered (black lines in graphs). This means that *chlorophyll a* pick up further away than the Somalia upwelling is responsible for this. MSAM and $DMSO_2$ are low or not detected during leg 1, therefore chlorophyll exposure in regions further away than the Somalia upwelling does not appear to play a role. The calculations in leg 2 are generally quite similar and therefore independent of the weighting parameter p.

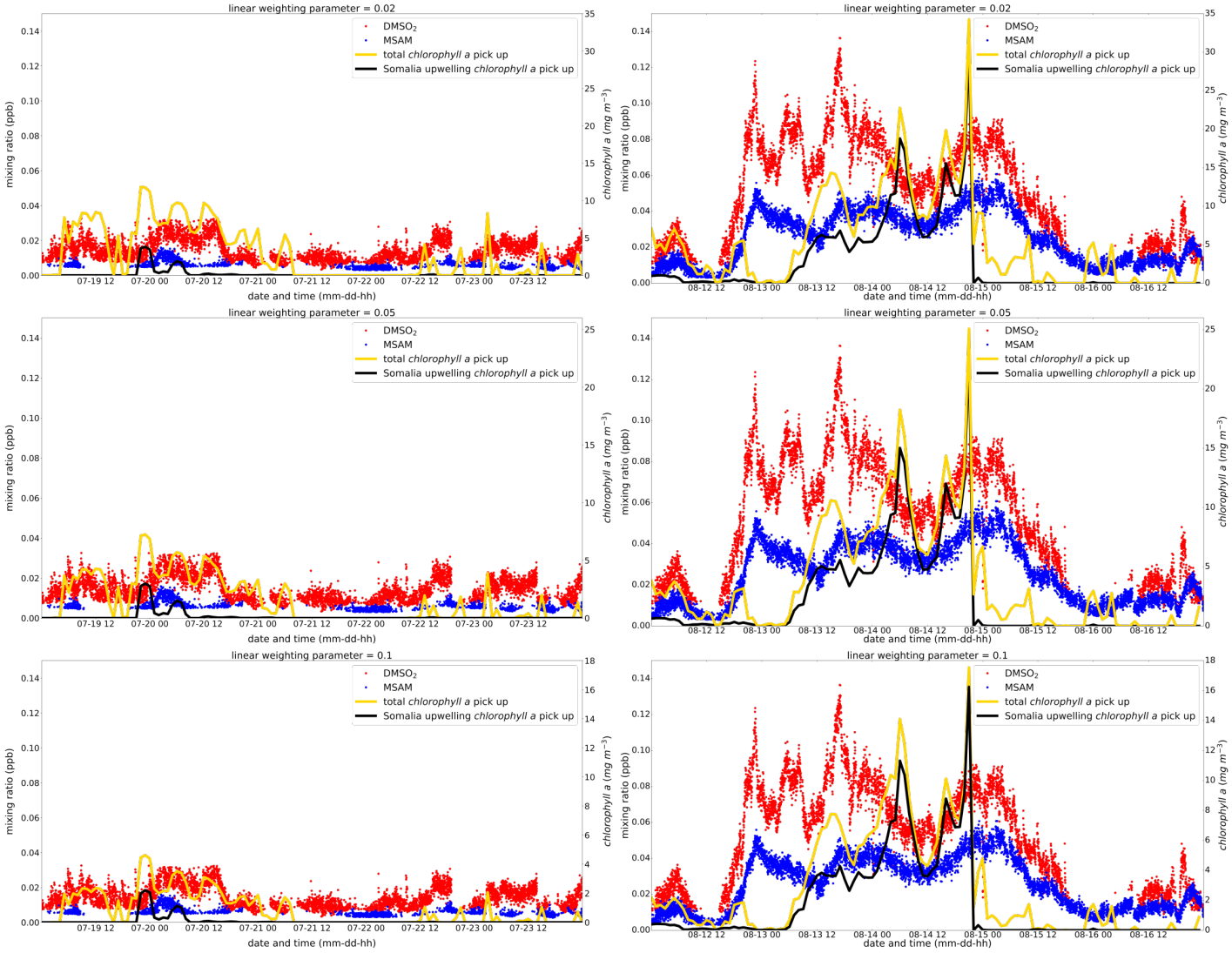

Figure S1: Linear weighting parameters from $p = 0.02 - 0.1$. The total *chlorophyll a* exposure (yellow line) and the *chlorophyll a* exposure originating from the Somalia upwelling region (black line) is plotted. The corresponding y-axis for the *chlorophyll a* exposure is displayed on the right side. Measured ambient mixing ratios in ppb for $DMSO_2$ and MSAM are plotted in red and blue with the corresponding y-axis on the left side. In the left column leg 1 and in the right column leg 2 is displayed.

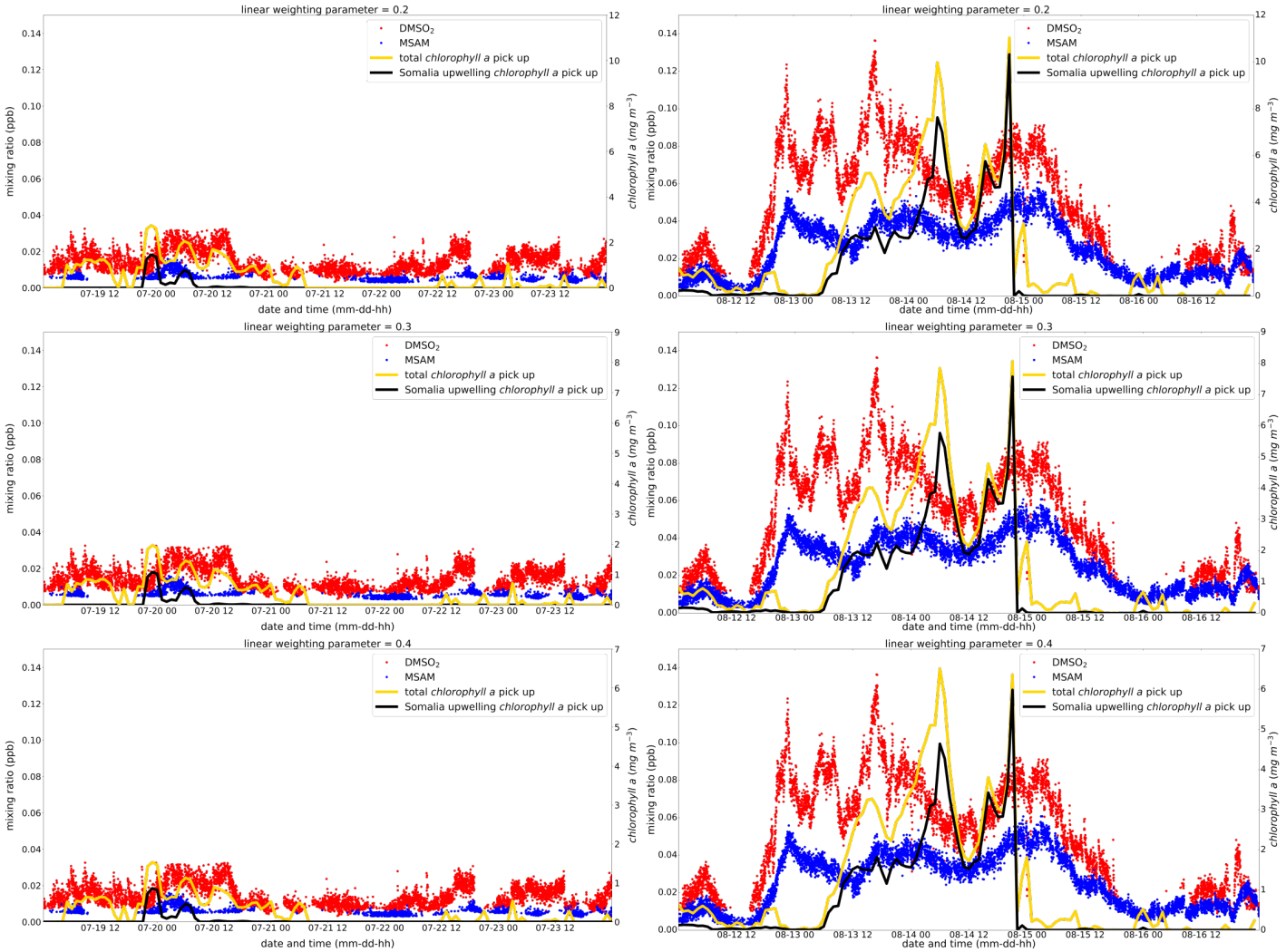

Figure S2: Linear weighting parameters from $p = 0.2-0.4$. The total *chlorophyll a* exposure (yellow line) and the *chlorophyll a* exposure originating from the Somalia upwelling region (black line) is plotted. The corresponding y-axis for the *chlorophyll a* exposure is displayed on the right side. Measured ambient mixing ratios in ppb for $DMSO_2$ and MSAM are plotted in red and blue with the corresponding y-axis on the left side. In the left column leg 1 and in the right column leg 2 is displayed.

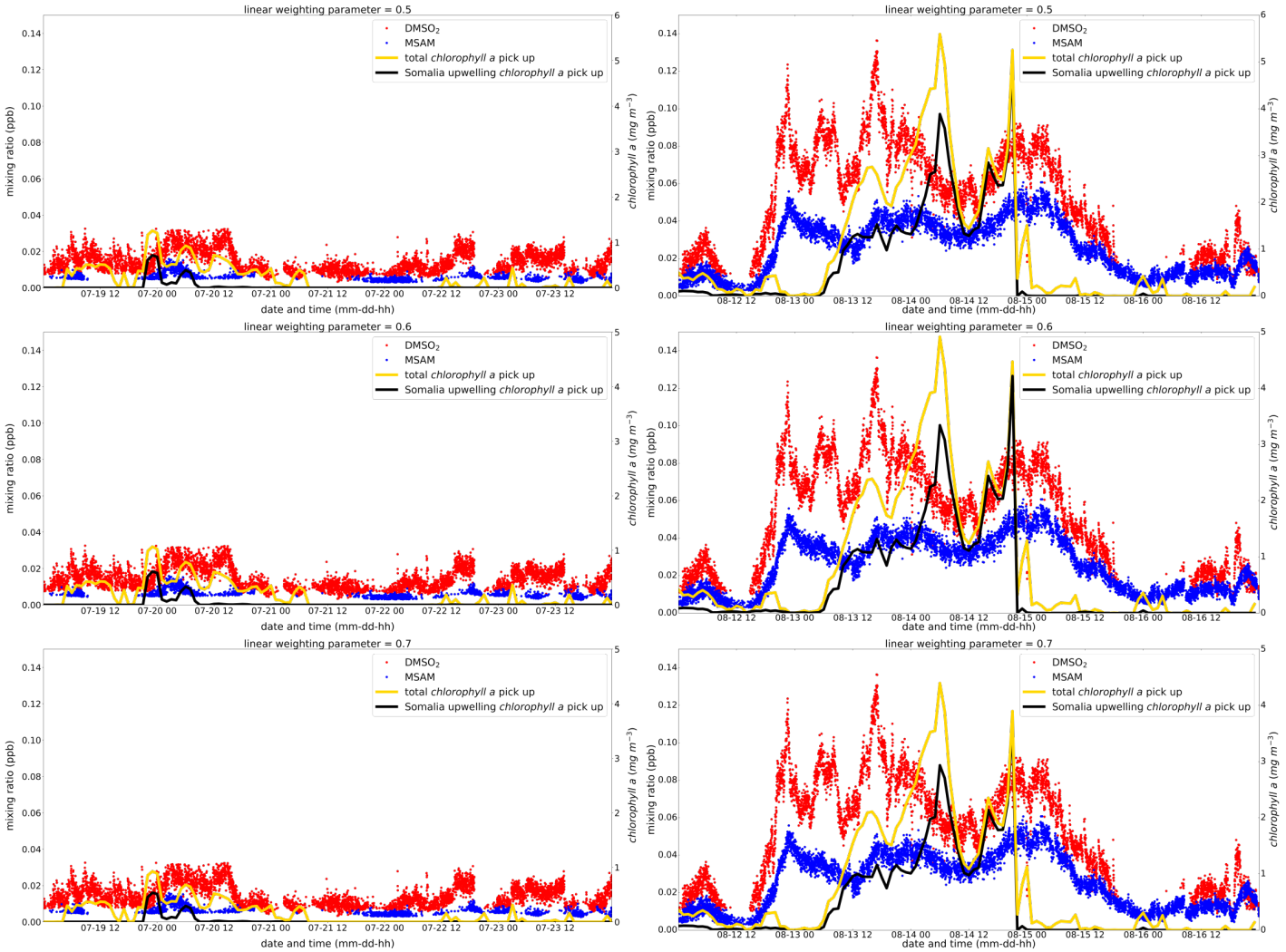

Figure S3: Linear weighting parameters from $p = 0.5-0.7$. The total *chlorophyll a* exposure (yellow line) and the *chlorophyll a* exposure originating from the Somalia upwelling region (black line) is plotted. The corresponding y-axis for the *chlorophyll a* exposure is displayed on the right side. Measured ambient mixing ratios in ppb for $DMSO_2$ and MSAM are plotted in red and blue with the corresponding y-axis on the left side. In the left column leg 1 and in the right column leg 2 is displayed.

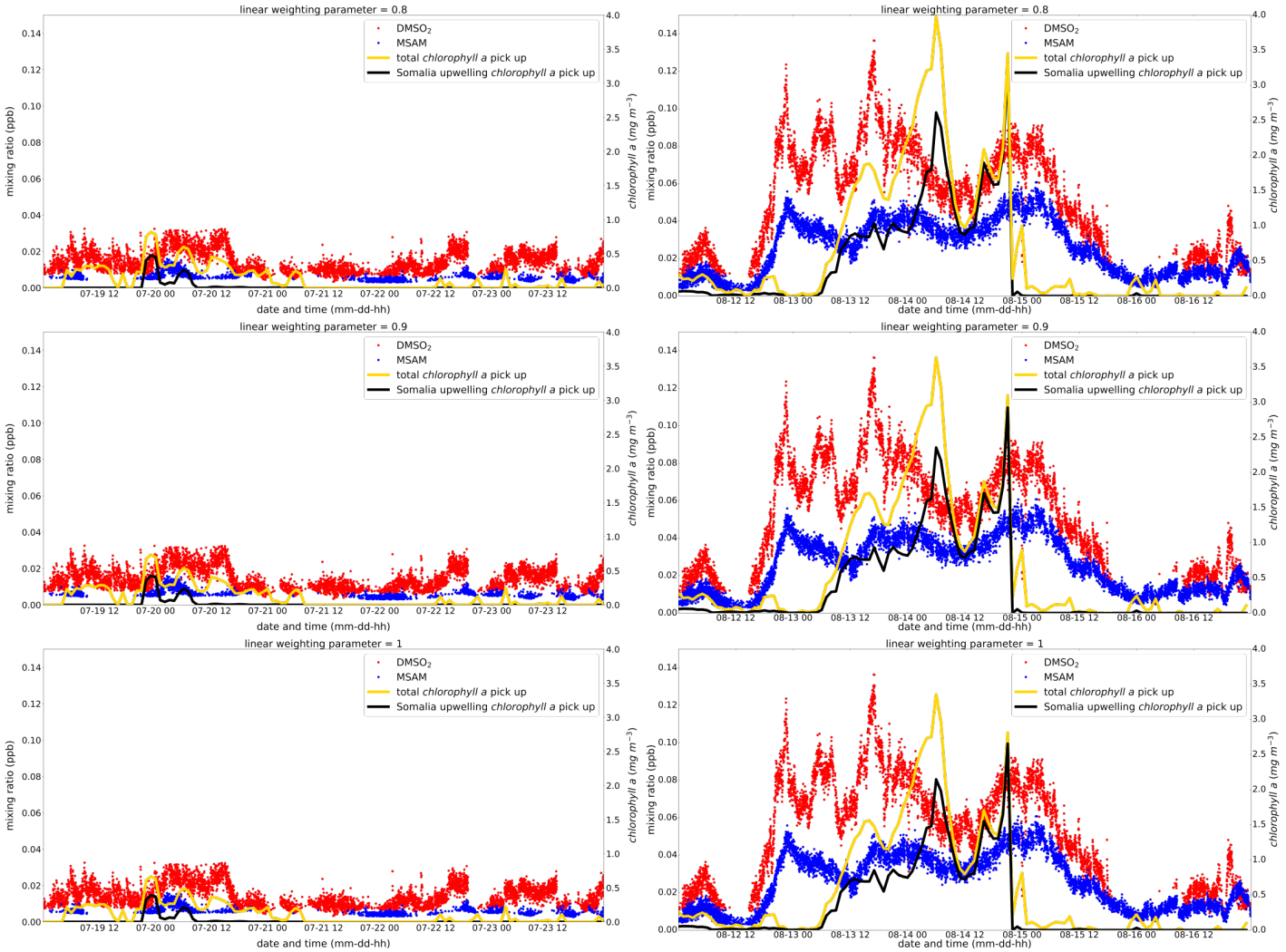

Figure S4: Linear weighting parameters from $p = 0.8 - 1$. The total *chlorophyll a* exposure (yellow line) and the *chlorophyll a* exposure originating from the Somalia upwelling region (black line) is plotted. The corresponding y-axis for the *chlorophyll a* exposure is displayed on the right side. Measured ambient mixing ratios in ppb for $DMSO_2$ and MSAM are plotted in red and blue with the corresponding y-axis on the left side. In the left column leg 1 and in the right column leg 2 is displayed.

3.2 Exponential weighting factors

The exponential weighting factor has the form $w_{exp} = p^t$, p, where p is the weighting parameter and t is the number of hours before arrival at the ship's location. The weighting factor is then multiplied with the respective *chlorophyll a* water content to yield the weighted *chlorophyll a*. The weighting parameter was varied from $p = 0.8$ to $p = 0.99$ (see Fig. S5 till Fig. S8). A weighting parameter of 1 means that all *chlorophyll a* water content is weighted equally. If p is close to 1 we see in the first leg a small increase in total *chlorophyll a* exposure coming from *chlorophyll a* pick up further away as the Somalia upwelling (as for the linear case). For the other cases we see in leg 2 that the Somalia upwelling region always constitutes the mayor part of the total *chlorophyll a* exposure, even in the case of $p = 0.8$, which discriminates strongly against chlorophyll exposure further away from the ship.

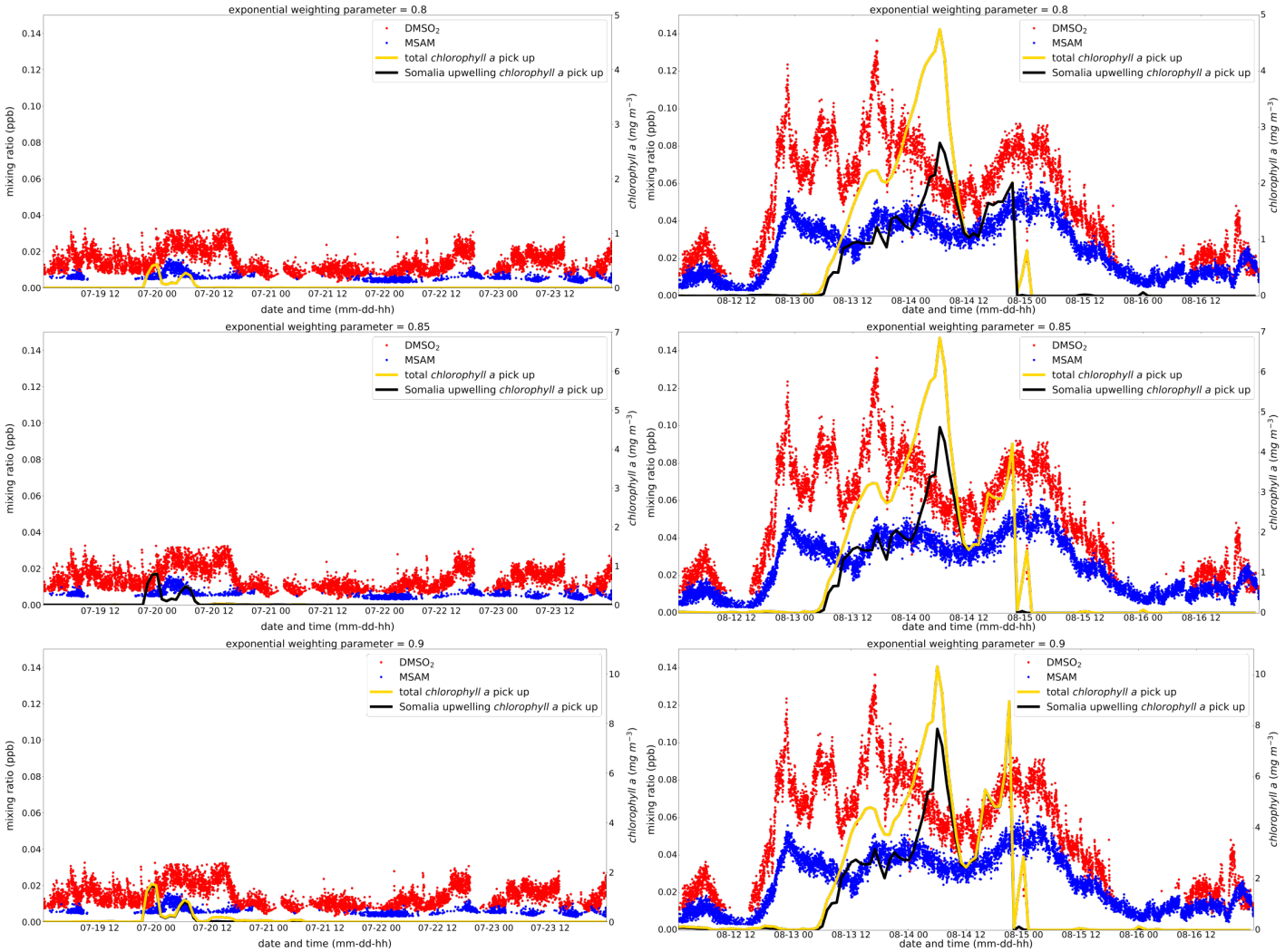

Figure S5: Exponential weighting parameters from $p = 0.8 - 0.9$. The total *chlorophyll a* exposure (yellow line) and the *chlorophyll a* exposure originating from the Somalia upwelling region (black line) is plotted. The corresponding y-axis for the *chlorophyll a* exposure is displayed on the right side. Measured ambient mixing ratios in ppb for $DMSO_2$ and MSAM are plotted in red and blue with the corresponding y-axis on the left side. In the left column leg 1 and in the right column leg 2 is displayed.

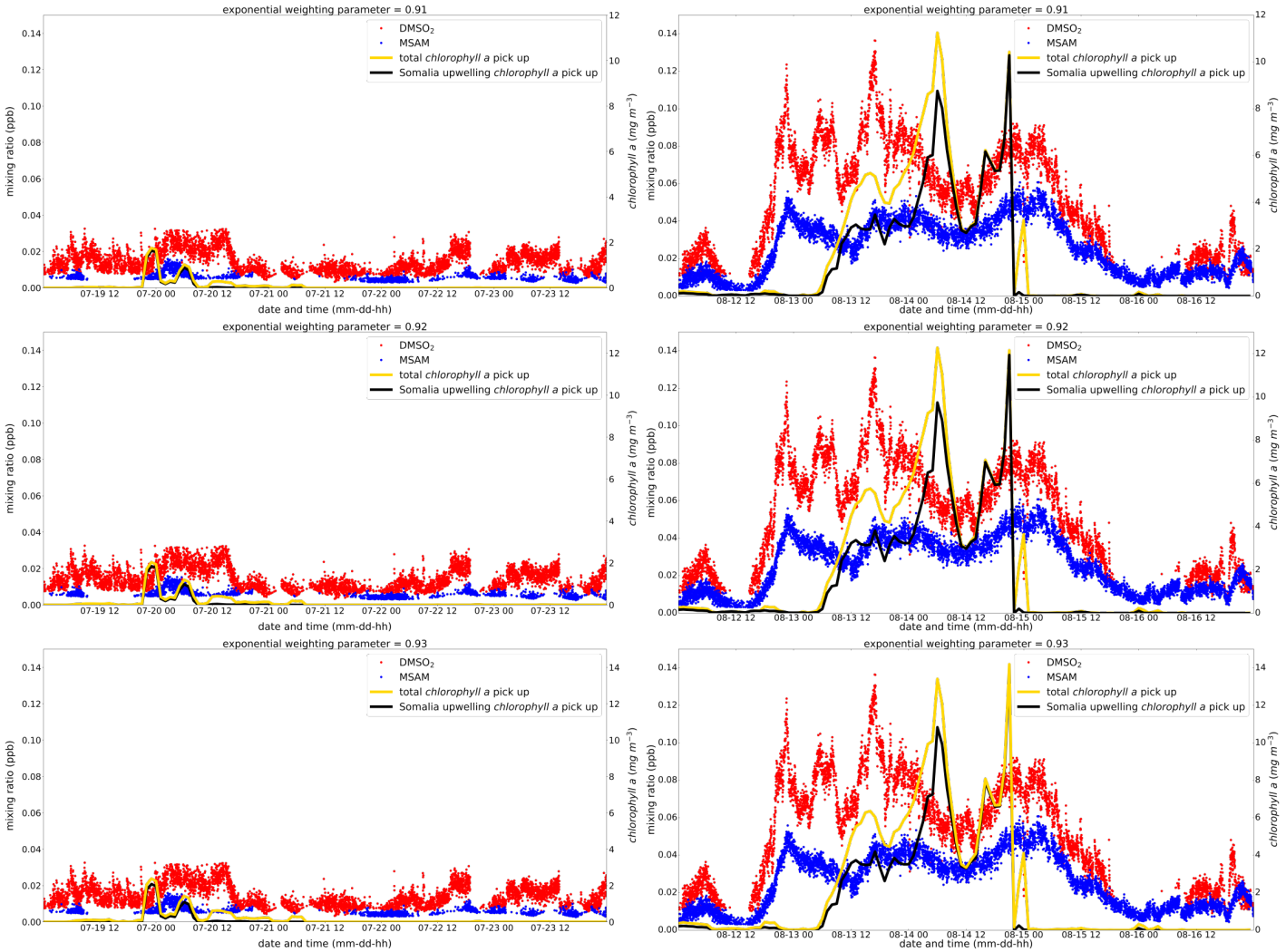

Figure S6: Exponential weighting parameters from $p = 0.91 - 0.93$. The total *chlorophyll a* exposure (yellow line) and the *chlorophyll a* exposure originating from the Somalia upwelling region (black line) is plotted. The corresponding y-axis for the *chlorophyll a* exposure is displayed on the right side. Measured ambient mixing ratios in ppb for $DMSO_2$ and MSAM are plotted in red and blue with the corresponding y-axis on the left side. In the left column leg 1 and in the right column leg 2 is displayed.

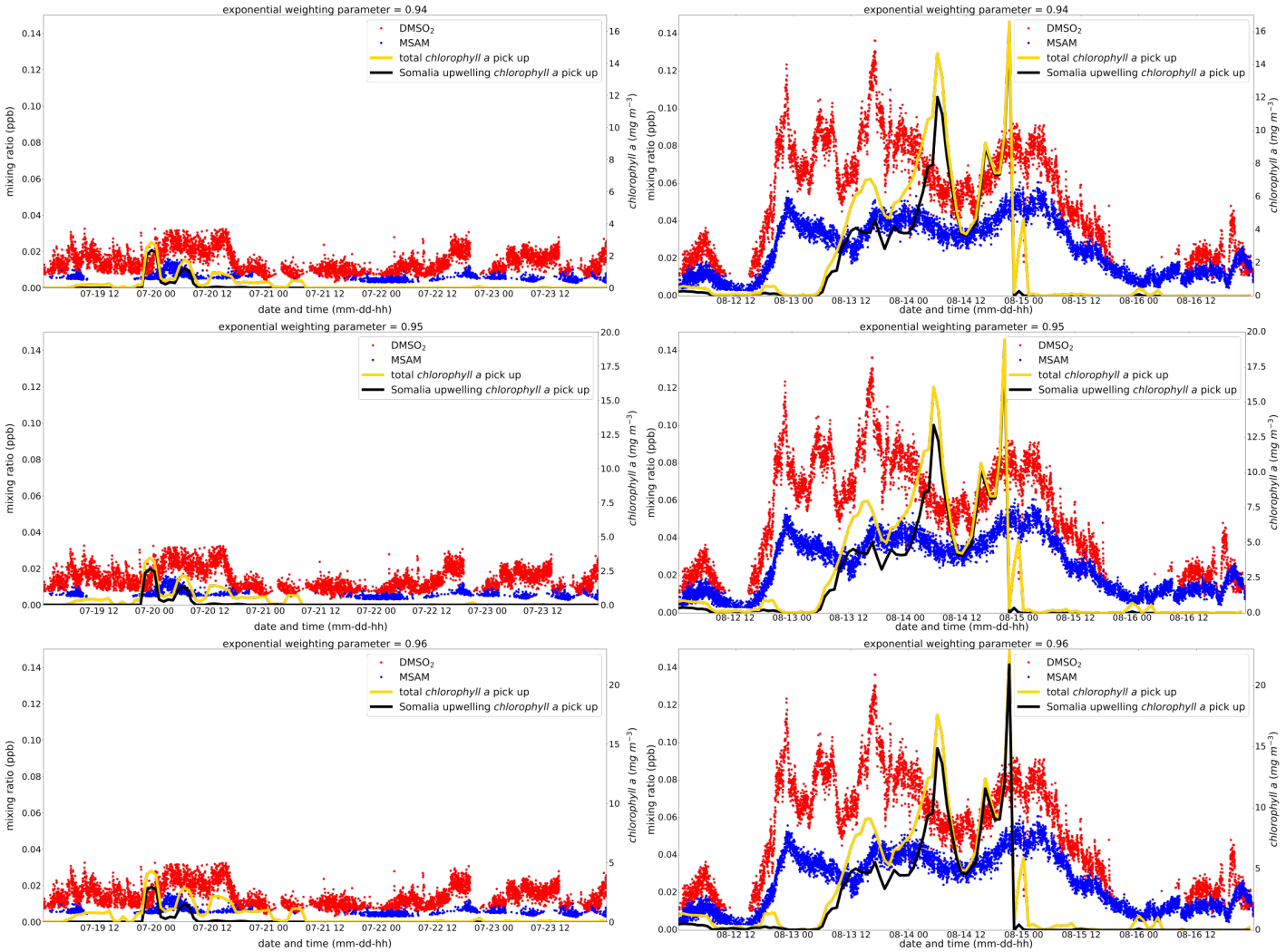

Figure S7: Exponential weighting parameters from $p = 0.94 - 0.96$. The total *chlorophyll a* exposure (yellow line) and the *chlorophyll a* exposure originating from the Somalia upwelling region (black line) is plotted. The corresponding y-axis for the *chlorophyll a* exposure is displayed on the right side. Measured ambient mixing ratios in ppb for $DMSO_2$ and MSAM are plotted in red and blue with the corresponding y-axis on the left side. In the left column leg 1 and in the right column leg 2 is displayed.

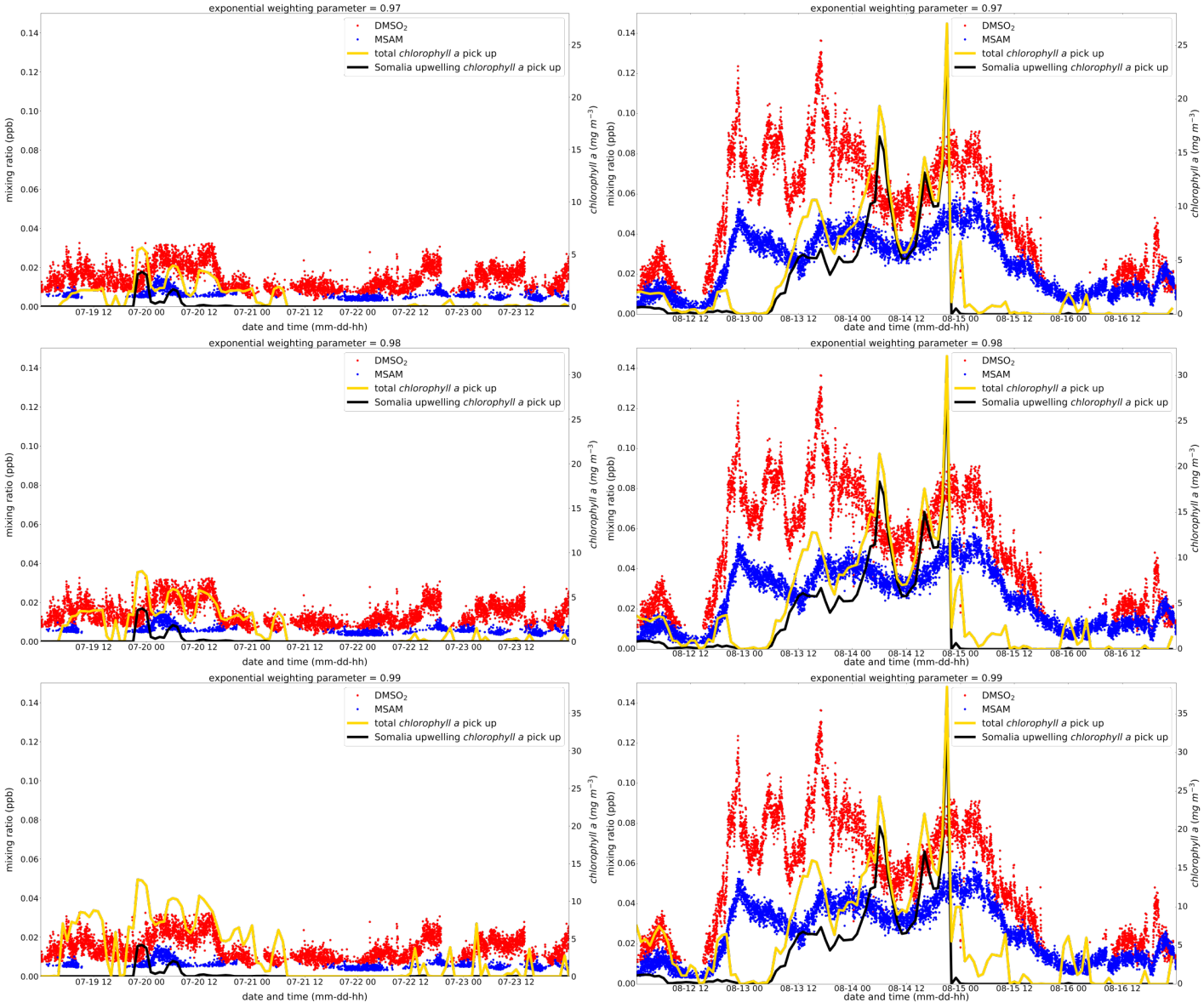

Figure S8: Exponential weighting parameters from $p = 0.97 - 0.99$. The total *chlorophyll a* exposure (yellow line) and the *chlorophyll a* exposure originating from the Somalia upwelling region (black line) is plotted. The corresponding y-axis for the *chlorophyll a* exposure is displayed on the right side. Measured ambient mixing ratios in ppb for $DMSO_2$ and MSAM are plotted in red and blue with the corresponding y-axis on the left side. In the left column leg 1 and in the right column leg 2 is displayed.

4 Diel variability plots

Diel variability of DMS, $DMSO_2$ and MSAM was calculated using only days when the wind was coming from the Somalia upwelling region. For whole days this only occurred on the 13th and 14th of August. On the 12th of August MSAM and $DMSO_2$ only started to increase and on the 15th they started to decline. The relatively short duration of the dataset available for diel variability calculations (2 days), taken on a moving platform means that variations can be interpreted as diel variations (driven by emission or atmospheric removal) or as source variations. Conclusions drawn from these plots should be treated with caution.

DMS seems to be higher at night than during the day (see Fig. S9 (a)). That is expected under stable conditions as DMS gets oxidized during daytime with OH.

$DMSO_2$ shows a tendency to be lower during daytime than at night (see Fig. S9 (b)). After sunset there is an increase in $DMSO_2$ which could hint at formation via NO_3 from the remaining DMSO concentrations.

MSAM we suggest is produced in the waters of the Somalia upwelling not in the atmosphere and subsequently transported to the ship. The time it took airmasses from the Somalia upwelling to reach the ship was 10 h to a day on the 13th and around 4 h on the 14th of August. So if we roughly assume an average travel time of 10 h for the diel cycle we have to shift the solar irradiation by 10 hours to the left (see orange filled curve in S9 (c)) in order to get the solar irradiation at the time of release from the Somalia upwelling. This hints at a production of MSAM in relation with photosynthetic activity since the higher values of MSAM occur together with higher solar irradiation in the Somalia upwelling region.

But as already stated above other effects like changes in transport time from the Somalia upwelling due to changes in wind speed and ship movement could have played a more important role.

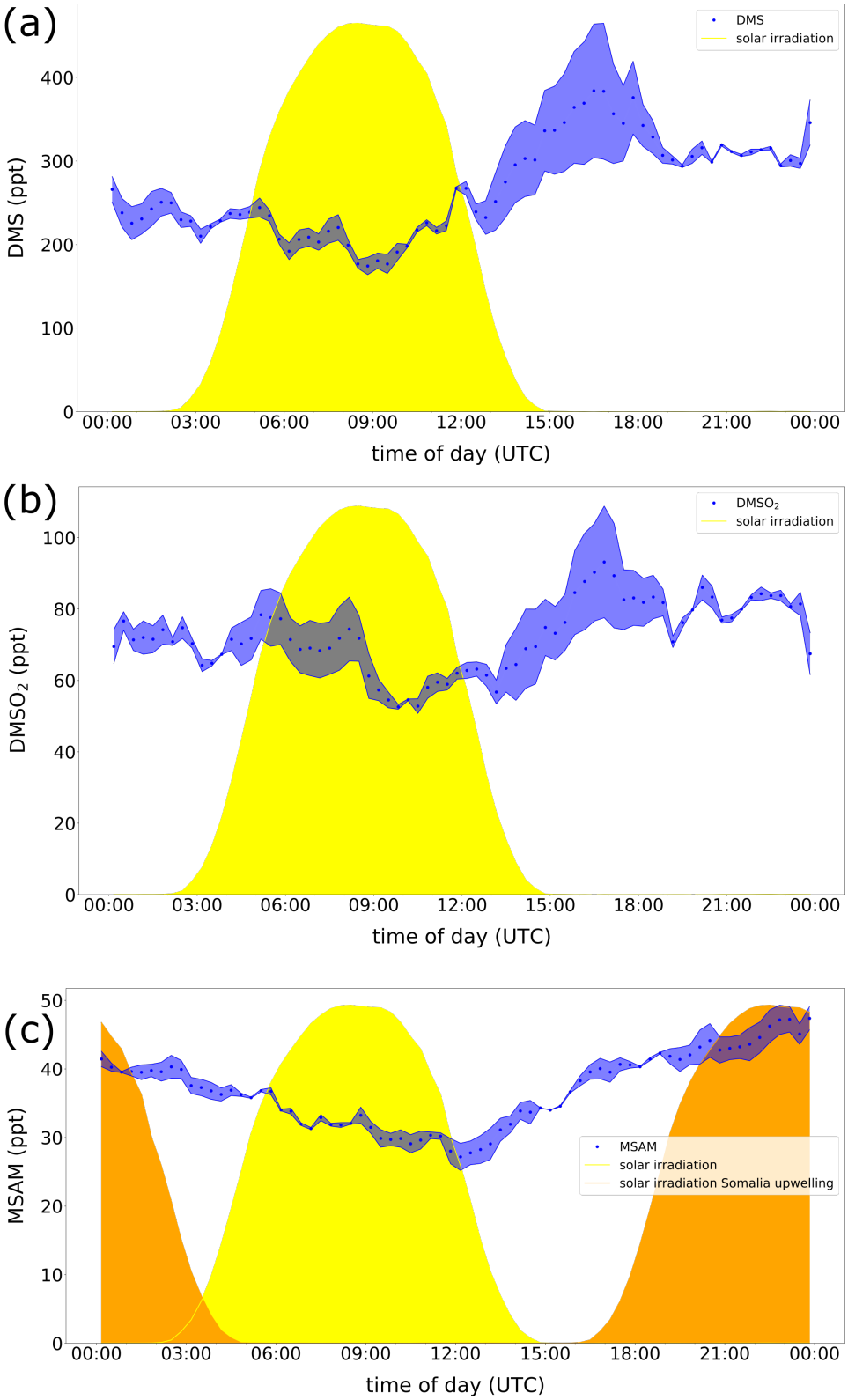

Figure S9: Diel variability of DMS (a), $DMSO_2$ (b) and MSAM (c). The blue dots are the mean and the light blue shading represents the 25th to 75th percentile. The yellow filled curve represents the solar irradiation. The diel variability was calculated using only days when the wind was coming the whole time from the Somalia upwelling region. Therefore we could only used the 13th and 14th of August for this calculations. The orange filled curve in (c) is the solar irradiation at the Somalia upwelling at the time of release of MSAM (assuming an average travel time of 10 h).

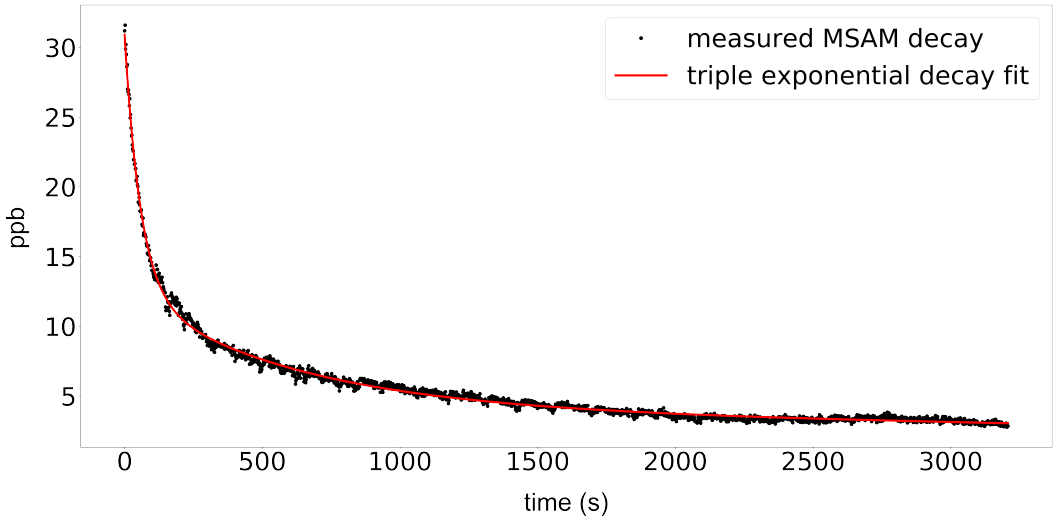

Figure S10: Measurement of the resulting time series of a step change in MSAM concentration. At $t = 0$ a 100 sccm flow of a stable MSAM concentration is replaced by clean zero air with the same humidity and flow. The resulting decay curve (black) is fitted with a triple exponential decay function (red).

5 Inlet characterization

We induced a concentration step change in order to determine the e-folding time (time it takes for a value to decay to 1/e) for an 1/8" teflon tubing inlet of 0.4 m length. An air flow of 100 sccm with a stable MSAM concentration was replaced by an air flow without MSAM (same flow and humidity). The resulting time series response (see Fig. S10) is an exponential decay which does not necessarily follow a single exponential decay [6]. A single exponential decay fit is not able to accurately fit the measured decay signal. We employed a triple exponential decay function to fit the signal $S(t)$ (see equation 6). In this equation the parameters a, b and c added together will give the concentration at $t = 0$ and the parameters τ_a, τ_b and τ_c are the decay timescales. The timescale τ gives the time it takes for the signal to drop to 1/e (e-folding time). The results of the fit yield $a = 18.3$, $b = 8.2$ and $c = 4.4$ (unit is ppb) with $\tau_a = 58$, $\tau_b = 581$ and $\tau_c = 8561$ (unit is seconds). This means that the observed exponential decay has different timescale regimes. First it decays quickly with a timescale of around one minute, then this increases to 10 minutes up to a timescale of around 142 minutes. To a good estimate the decay timescales depend proportionally on tubing length and diameter and inversely on the flow rate and saturation concentration [7]. On this basis we can estimate the decay timescales of our AQABA inlet setup (length 10 m, 1/2" Teflon tubing, flow of 3 slpm) to 3.3 minutes, 33 minutes and 8 hours. Therefore concentration changes happening even on timescales of half an hour or longer will be smoothed, i.e. the real variance of the concentration might have been considerably larger.

$$S(t) = a * e^{-\frac{t}{\tau_a}} + b * e^{-\frac{t}{\tau_b}} + c * e^{-\frac{t}{\tau_c}} \tag{6}$$

6 Synthesis of MSAM

The partitioning of MSAM to the inside wall of the Teflon tubing raises the question whether the observed MSAM could be generated there on surfaces. No inlet test was done during the campaign to address this issue since this discovery was a surprise. Therefore, we cannot rule out that such an effect occurs. However we do consider it unlikely that MSAM was formed via a surface reaction of $DMSO_2$ (or an analogous species) with NH_3 or NH_4^+ . $DMSO_2$ as well as NH_3 and NH_4^+ are both very unreactive molecules. Additionally, we see no way of how NH_4^+ and NH_3 could lose their hydrogen atoms in order to form the requisite NH_2 group. A chemical synthesis pathway for sulfonamides from sulfonic acids has been published [2]. The first step towards

the production of MSAM would be removal of the whole OH group of methane sulfonic acid (MSA), creating a $CH_3SO_2^+$ ion. In an aqueous solution, the preferred reaction is, however, the removal of H^+, i.e. forming $CH_3SO_3^-$.
In this chemical synthesis, aggressive reagents such as trichlorotriazine and high energy (e.g. from a microwave) are used to create an intermediate CH_3SO_2Cl which reacts as a $CH_3SO_2^+$ ion. In the second step, this $CH_3SO_2^+$ ion reacts with an amine (for MSAM formation this would need to be replaced by NH_3) in a strong basic solution (NaOH(aq)), abstracting an H from NH_3 to form MSAM. The fact that sulfonic acids and not sulfones are used as precursors in synthesis of sulfonamides points out that formation from sulfones is either not possible or more difficult than with sulfonic acids. Formation of MSAM therefore needs aggressive reagents, input of energy and strong basic conditions which were not present in our inlet. We are not aware of any other possible pathways which could form MSAM in our inlet. However we cannot rule it out completely, thus it remains a uncertainty that future studies should clarify.

7 MSAM concentration in seawater

We cannot provide an accurate calculation for the waterside concentration required as the physical conditions in the Somalia upwelling region are not known and the Henry's law constant is uncertain. Calculation of the water concentration needed to support measured atmospheric concentrations of MSAM would require a model. Due to the lack of knowledge of the conditions at the upwelling region we consider that not feasible.
However from equation 1 we can calculate the minimum MSAM water concentration (A) required to produce a positive flux to the atmosphere at a given atmospheric concentration (G). Due to the high Henry's law constant (H) compared e.g. to DMS it has to be expected that, with this two-layer model, MSAM water concentrations have to be considerably larger than DMS water concentrations in order to produce a flux to the atmosphere. Concentrations higher than $A = G * H$ will result in a flux to the atmosphere. The water side concentration (for G =50 ppt and $H = 3.3 \times 10^4$ M atm^{-1}) needs to be higher than 1700 nM. This appears very high in comparison with previously reported water phase concentration of VOC [8, 4]. Measurements of water concentrations together with ambient air measurements of MSAM in an upwelling region are needed to better understand the ocean air exchange of MSAM.

References

[1] W. J. de Bruyn, Jeffrey A. Shorter, P. Davidovits, D. R. Worsnop, M. S. Zahniser, and C. E. Kolb. Uptake of gas phase sulfur species methanesulfonic acid, dimethylsulfoxide, and dimethyl sulfone by aqueous surfaces. *Journal of Geophysical Research: Atmospheres*, 99(D8):16927–16932, 1994.

[2] Lidia de Luca and Giampaolo Giacomelli. An easy microwave-assisted synthesis of sulfonamides directly from sulfonic acids. *The Journal of organic chemistry*, 73(10):3967–3969, 2008.

[3] B. B. Hicks and P. S. Liss. Transfer of so2 and other reactive gases across the air—sea interface. *Tellus*, 28(4):348–354, 1976.

[4] A. Lana, T. G. Bell, R. Simó, S. M. Vallina, J. Ballabrera-Poy, A. J. Kettle, J. Dachs, L. Bopp, E. S. Saltzman, J. Stefels, J. E. Johnson, and P. S. Liss. An updated climatology of surface dimethlysulfide concentrations and emission fluxes in the global ocean. *Global Biogeochemical Cycles*, 25(1):n/a–n/a, 2011.

[5] P. S. Liss and P. G. Slater. Flux of gases across the air-sea interface. *Nature*, 247(5438):181–184, 1974.

[6] Xiaoxi Liu, Benjamin Deming, Demetrios Pagonis, Douglas A. Day, Brett B. Palm, Ranajit Talukdar, James M. Roberts, Patrick R. Veres, Jordan E. Krechmer, Joel A. Thornton, Joost A. de Gouw, Paul J. Ziemann, and Jose L. Jimenez. Effects of gas–wall interactions on measurements of semivolatile compounds and small polar molecules. *Atmospheric Measurement Techniques*, 12(6):3137–3149, 2019.

[7] Demetrios Pagonis, Jordan E. Krechmer, Joost de Gouw, Jose L. Jimenez, and Paul J. Ziemann. Effects of gas–wall partitioning in teflon tubing and instrumentation on time-resolved measurements of gas-phase organic compounds. *Atmospheric measurement techniques*, 10(12):4687–4696, 2017.

[8] Cathleen Schlundt, Susann Tegtmeier, Sinikka T. Lennartz, Astrid Bracher, Wee Cheah, Kirstin Krüger, Birgit Quack, and Christa A. Marandino. Oxygenated volatile organic carbon in the western pacific convective center: ocean cycling, air–sea gas exchange and atmospheric transport. *Atmospheric Chemistry and Physics*, 17(17):10837–10854, 2017.

[9] S. E. Schwartz. Factors governing dry deposition of gases to surface-water. In S. E. Schwartz and W. G.N. SLINN, editors, *PRECIPITATION SCAVENGING AND ATMOSPHERE-SURFACE EXCHANGE, VOLS 1-3*, pages 789–801, NEW YORK, 1992. HEMISPHERE PUBL CORP.

[10] M. Yang, R. Beale, P. Liss, M. Johnson, B. Blomquist, and P. Nightingale. Air–sea fluxes of oxygenated volatile organic compounds across the atlantic ocean. *Atmospheric Chemistry and Physics*, 14(14):7499–7517, 2014.